High rate capability of coconut kernel derived carbon as an anode material for lithium-ion batteries

Tirupathi Rao Penki[1], D. Shanmughasundaram[1], Brij Kishore[1] and N. Munichandraiah[1,2*,]

[1]*Department of Inorganic and Physical Chemistry, Indian Institute of Science, Bangalore 560012, India*
[2]*Energy Storage and System Initiative Center, Indian Institute of Science, Bangalore 560012, India*

[*]Corresponding author. Tel: (+91) 80 22933183; E-mail: muni@ipc.iisc.ernet.in

ABSTRACT

Carbon has been prepared by pyrolysis of grated, milk-extracted coconut kernel at 600 $^{\circ}$C under nitrogen atmosphere. The disordered carbon has sheet like morphology. The carbon exhibits a high reversible Li$^+$ intercalation capacity in a non-aqueous electrolyte. The initial charge and discharge capacities are 990 and 400 mAh g^{-1}, thus resulting in an irreversible capacity loss of 590 mAh g^{-1}. Nevertheless, subsequent discharge capacity is stable over a large number of charge-discharge cycles. The electrodes withstand charge-discharge currents as high as 1257 mA g^{-1} and they deliver discharge capacity of 80 mAh g^{-1}. Diffusion coefficient of Li$^+$ obtained from galvanostatic intermittent titration is 6.7 x 10^{-12} cm^2 s^{-1}. Thus the coconut kernel derived carbon is a suitable anode material for Li-ion batteries. Copyright © 2014 VBRI press.

Keywords: Coconut kernel carbon; Li-ion cells; charge-discharge cycling; high rate capability.

Tirupathi Rao Penki completed his under graduation from S. A. S Govt. College Narayanapuramand post-graduation from School of Chemistry, Andhra University, Visakhapatnam. At present he is pursuing his doctoral degree at Department of Inorganic and Physical Chemistry, Indian Institute of Science, Bangalore under the supervision of Prof N. Munichandraiah in the field of nanostructure materials for Li-ion battery.

D. Shanmughasundaram completed his B.Sc. from ChikkaiahNaicker College, Erode and M.Sc. Chemistry from Erode Arts & Science College, Bharathiar University, Coimbatore. Currently he is working under the supervision of Prof N. Munichandraiah Department of Inorganic and Physical Chemistry, Indian Institute of Science Bangalore. His field of interest is materials for Li-ion batteries, thin film batteries and supercapacitors.

N. Munichandraiah obtained his M.Sc. degree from Sri Venkateswara University, Tirupati and Ph.D. degree from Indian Institute of Science, Bangalore. He is presently Professor in the Department of Inorganic and Physical Chemistry, Indian Institute of Science, Bangalore. His research of interests is mainly Li-ion and Li-air batteries, supercapacitors, conducting polymers, electrocatalysis and photoelectrolysis.

Introduction

Reversible electrochemical processes of insertion and extraction of Li in carbonaceous materials are key processes for the successful development of rechargeable Li-ion batteries in recent years. Problems arising from Li metal as the negative electrode for rechargeable non-aqueous batteries could be overcome by using carbon in place of Li metal. Layered structure of graphite with inter-layer Van der Waals gap, where Li$^+$ ions are accommodated, is the primary property responsible for this success, thus carbon becoming one of the advanced energy material [1-3]. Although natural graphite is extensively studied for electrochemical properties in connection with intercalation/de-intercalation of Li, several other disordered carbon materials are also studied for application in Li-ion batteries [2]. The non-graphitic materials include petroleum coke [4], carbons prepared from phenolic resins [5], phenol-formaldehyde resins [6], poly(p-phenylene) [7], poly(acrylonitrile) [8], poly(vinyl chloride) [9], carbon nanotubes [10], etc. Carbonaceous materials prepared from agricultural sources such as sugar [11-14], rice husk [15, 16], potato starch [17], banana fibers [18], coffee shells [19], peanut shells [20] and coconut shells [21] form an interesting class of carbons, which are also studied for Li-ion battery applications. These carbons are considered as green-carbons. Although coconut shell based carbons are extensively prepared, there are no reports on coconut kernel as the source for carbon. The kernel is fibrous in nature and

therefore the carbon obtained from it is expected to be fibrous or layered.

The aim of the present study is to prepare carbon from coconut kernel as the source and investigate its properties as the anode material of Li-ion battery. Milk is extracted from coconut kernel and the pulp which is free from milk is used for preparation of carbon at a temperature as low as 600 $^{\circ}$C. Due to relatively low carbonization temperature, the product exhibits disordered structure and contains significant amount of hydrogen. The carbon has high Li^+ intercalation capacity with high rate capability.

Experimental

Materials

Materials and high purity chemicals used in the experiments are as follows: well ripened raw coconuts from a vegetable market, acetylene black (Alfa Aesar, USA), polyvinylidine fluoride (PVDF, Aldrich, USA), n-methyl pyrrolidinone (NMP, Aldrich, USA), Copper foil (India), lithium metal foil (Aldrich, USA) commercial electrolyte of 1M LiPF6 dissolved in ethylene carbonate, diethyl carbonate and dimethyl carbonate (2:1:2 v/v) (Chameleon, Japan), acetone (India), HNO_3 (SD fine chemicals, India) homemade double-distilled water prepared in all quartz distillation unit was used whenever required.

Methods

Kernel from well-ripened coconuts was grated and milk was extracted by grinding repeatedly in warm water using a kitchen grinding machine. The pulp was washed thrice in double distilled water under stirring, finally rinsed with a mixture of double-distilled water and acetone (1:1 by volume), and dried at 120 $^{\circ}$C for 12 h. Carbonization of the dried kernel (300 mg) was carried out under N_2 atmosphere at 600 $^{\circ}$C for 3 h in a home-made tubular furnace, which was heated from room temperature at a rate of 10 $^{\circ}$C min^{-1}. The sample was cooled to ambient temperature under N_2 flow, and subjected to grinding in a mortar. The quantity of carbon obtained in a batch was about 100 mg. Carbons were prepared in several batches and mixed together for further studies.

For fabrication of electrodes, carbon (80 wt%), acetylene black (15 wt%) and PVDF (5 wt%) were mixed in a mortar and a few drops of NMP were added to obtain a slurry. The slurry was applied on a copper foil (12 mm diameter) and dried at 120 $^{\circ}$C under vacuum for 12 h. The Cu foil (thickness 0.2 mm) was polished to a smooth finish by successive grades of emery, washed thoroughly, etched in dilute HNO_3, washed again with double distilled water, rinsed in acetone and air dried before using as the substrate. The mass of active material coated on Cu foil was 3-5 mg cm^{-2}. Lithium metal foil (0.38 mm thickness) was used as a counter-cum-reference electrode and absorbing glass mat was used as a separator. A commercial electrolyte of 1M $LiPF_6$ dissolved in ethylene carbonate, diethyl carbonate and dimethyl carbonate (2:1:2 v/v) (Chameleon) was used as the electrolyte. Swagelok type cells were assembled in an argon filled MBraun glove box model Unilab. The cells were galvanostatically charged and discharged in the voltage range from 0.001 to 2.0 V at different current densities. Cyclic voltammetry and charge-discharge cycling

experimetns were carried out using a Biologic multi-channel potentiostat/galvanostat model VMP3. Galvanostatic intermittent titration technique (GITT) experiments were carried out using Solartron electrochemical interface model SI 1287. All experiments were carried out at 22 ± 2 $^{\circ}$C.

The carbon sample was characterized by powder X-ray diffraction (XRD) on a Philips X'Pert Pro diffractometer at 40 kV and 30 mA using Cu K$_\alpha$ (λ=1.5418 $\mathring{A}$) as the radiation source and the data are collected at 2θ ranging from 10 to 80° at a rate of 2° per min. Raman spectra were recorded using an In Via Raman spectrometer. The source of radiation was argon ion laser excited at 514 nm wavelength and 25 mV powers. The morphology was examined using a FEI Co scanning electron microscope (SEM) model Sirion and transmission electron microscope (TEM and HRTEM) model TECNAI-T20. Elemental analysis for C, H and N was carried out by using a Thermo Finnigan FLASH EA 1112 CHN analyzer. Nitrogen adsorption-desorption isotherms were recorded at -196 $^{\circ}$C by using Micromeritics surface area analyzer model ASAP 2020. The specific surface area was calculated by the Brunauer-Emmett-Teller (BET) method using the data in the relative pressure (p/p$_0$) range 0.05-0.25 from adsorption branch. The pore size distribution was calculated by Barrett-Joyner-Halenda (BJH) method from desorption branch of the isotherm.

Results and discussion

Physicochemical studies

The structural characterization of disordered carbons is generally based on powder XRD studies. Carbons prepared at low temperatures (500-1200 $^{\circ}$C) exhibit XRD patterns consisting of a few broad reflections corresponding to (002), (100) and (110) planes of graphite with rapidly decreasing intensity [22]. The origin of broad (002) reflection is interpreted as due to a small number of well stacked layers with a uniform interlayer distance (d$_{002}$) greater than that of graphite (3.35 Å). Powder XRD pattern of carbon prepared in the present study is shown in **Fig. 1**. It consists of two clear reflections at 2θ = 23 and 43° and another shallow reflection at 72°. All reflections are broad indicating disorder nature of the carbon. The 23, 43 and 72° reflections correspond to (002), (100) and (110) planes, respectively.
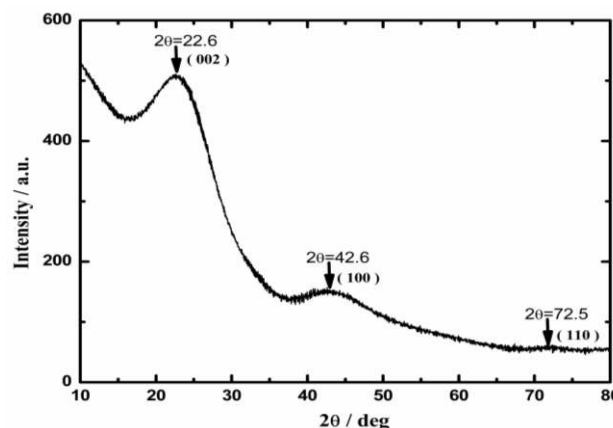

Fig. 1. Powder XRD pattern of carbon.

The XRD pattern is similar to the patterns reported by Dahn *et al* [23]. For cokes and soft carbons, only (002) and (004) reflections due to stacking of the layers are observed. The (100) and (110) reflections are attributed to inplane order [23]. The inter-layer spacing calculated from (002) plane (Fig. 1) is 3.80 Å, which is greater than the expected 3.35 Å for pure graphite [24]. It is known that the inter-graphene distance depends on the carbon source, the method of preparation and chemical treatment [11]. Inter-layer spacing values ranging from 3.77 to 4.10 Å are reported for various samples of carbon prepared from rice husk [15, 16]. A value of 4.07 Å is reported for spherical hard carbon prepared from potato starch [17]. The value obtained in the present study is within this range. Factors which affect the positions and widths of diffraction peaks include finite crystal size broadening, fluctuations in lattice parameters and strain [22]. Zhou *et al.* [22] reported structural abnormalities from micrographs of a coke carbon heated at 2800 $^\circ$C. Although the carbon layers were in parallel to one another, bending of layers and misalignments were visible at large. These imperfections increased when the treatment temperature was lowered. The high value of inter-layer spacing obtained in the present work is in agreement with this report [22]. Raman spectrum of carbon is shown in **Fig. 2**.
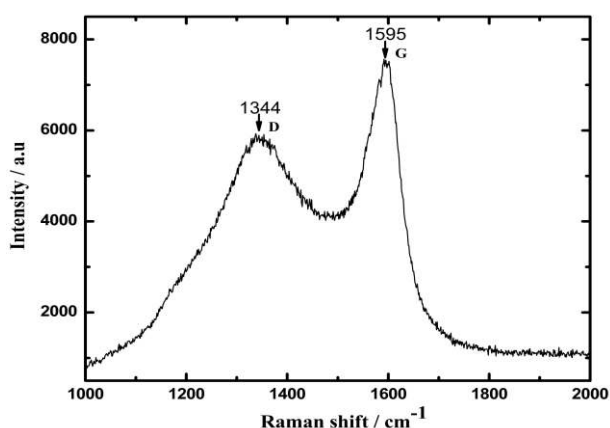

Fig. 2. Raman spectrum of carbon.

There are two bands at 1360 and 1580 cm^{-1}. Tuinstra and Koenig [25] studied Raman spectra of single crystals of graphite and other graphitic materials. Single crystals of graphite exhibited only a single line at 1575 cm^{-1}, whereas the other graphitic samples exhibited an additional line near 1355 cm^{-1}. The relative intensities of these two lines depended on the type of graphitic materials. The intensity of 1355 cm^{-1} line increased corresponding to an increase in the amount of unorganized carbon in the sample and also to a decrease in the crystal size. This line was attributed to Raman active modes of A_{1g} type [25]. The Raman line at 1575 cm^{-1} was present for all graphite samples studied [25]. A positive shift in frequency (~15 cm^{-1}) was observed in some samples with small crystal sizes. This band was attributed to E_{2g} mode of vibrations, which was restricted to the motion of atoms to the plane of the carbon atoms [25]. Additionally, there is a shoulder at ~1200 cm^{-1}, which may correspond to sp^3 carbon. Raman spectrum (**Fig. 2**) of carbon prepared in the present study agrees with spectra reported in [24, 25] for disordered carbon materials.

Scanning electron microscopy images (**Fig. 3A**) indicate that the coconut kernel carbon has micro-sheet like morphology, but wrinkled. This type of morphology is likely due to the fact that the raw material, namely coconut kernel, used for carbonization is fibrous in nature. When observed under higher magnification (**Fig. 3B**), a micro sheet of carbon is seen possessing layers stacked together.
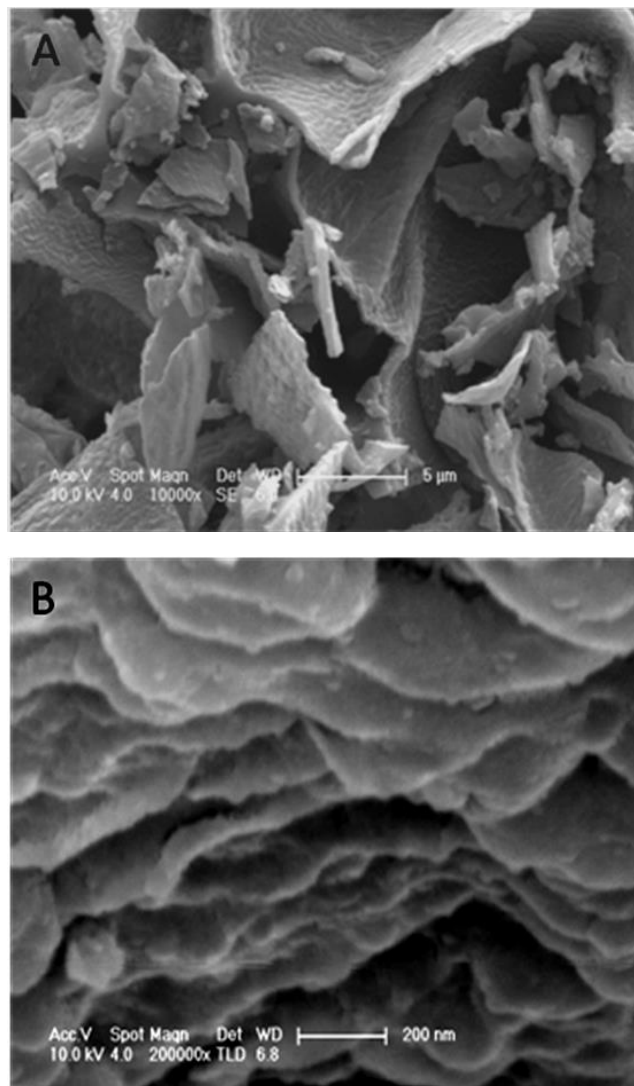

Fig. 3. SEM micrographs of carbon at different magnifications.

Tunneling electron microscopy images (**Fig. 4**) also suggest a sheet-like nano layers present one over the other. Yi *et al.* [26] synthesized nanosized disordered carbon from glucose by hydrothermal route and the product formed had spherical morphology. Carbon prepared from rubber at 600 $^\circ$C by Lin *et al*. [27] also has spherical morphology. Pillar-shaped morphology was reported for carbon prepared from a condensed aromatic compound [28]. Carbon prepared from potato starch consisted of spherical morphology [17]. In contrast to these reports, carbon prepared in the present study consists of layers which are stacked together. As the coconut kernel is fibrous in nature, it is thus inferred that the carbon prepared from it possesses layered morphology.

From N_2 adsorption-desorption isotherms, BET surface area of the carbon measured was 278 m^2 g^{-1}. Carbons generally used for Li$^+$ intercalation studies have similar surface area values. For instance, surface area of 230 m^2 g^{-1} was reported for polymethylacrylonitrile derived carbon [29]. From BJH curve of carbon prepared in the present study it was found that a broad spectrum of pores in the range 20-100 nm with a peak at 40 nm was present. From microanalysis, it was found that the carbon sample consists of C, H and N at 85.07, 2.69 and 3.01 wt% respectively. It is likely that about 10 wt% of impurities are present. Atomic ratio of C: H: N thus becomes 7.09: 2.69: 0.22. The small amount of N is due to the fact the carbonization was carried out in N_2 atmosphere. The H, originating from the hydrocarbons present in the kernel, is beneficial for the application of carbon for Li$^+$ ion insertion/de-insertion reactions. The atomic ratio of H/C thus becomes 0.38.
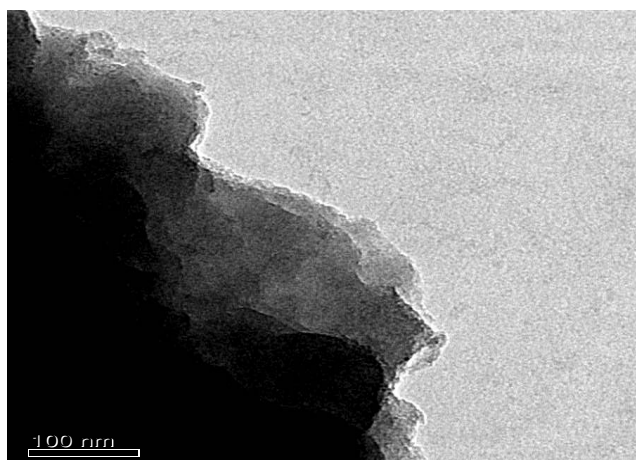
Fig. 4. TEM micrograph of carbon.

It is clear from the above physicochemical characterization studies that the low temperature calcination of milk-extracted coconut kernel produces a good quality carbon. As the milk was extracted from coconut kernel, all soluble constitutes are removed from the pulp. The carbon precursor essentially consists of water insoluble carbohydrates. During the process of carbonization in N_2 atmosphere, hydrogen and oxygen present in the kernel pulp are removed in the form of water, thus leaving behind essentially the carbon.

Electrochemical studies

Carbon electrode in non-aqueous electrolyte was subjected to cyclic voltammetry between 2.0 and 0.001 V (**Fig. 5**). In the first forward sweep from 2.0 V, there are broad current peaks at 1.2, 1.0, and 0.5 V. In the reverse sweep, broad humps are noticed at about 0.3 and 1.0 V (**Fig. 5**, curve 1). In the second forward sweep (**Fig. 5,** curve 2), the current decreases significantly in relation to curve 1, the broad current peaks are not clearly visible. Current during the reverse sweep decreases marginally in comparison with curve 1. The size of third repetitive voltammogram (**Fig. 5,** curve 3) is smaller than the preceding voltammograms.

Although cyclic voltammograms generally, throw light of electrochemical activity of battery electrode materials by displaying sharp or clear current peaks, voltammograms

reported for several carbons [27, 30-34] and also recorded in the present study do not have clear current peaks. Kim *et al*. [30] prepared hollow core-mesoporous shell carbon and recorded cyclic voltammograms between 2.5 and 0.0 V. In the first sweep, there was a broad cathodic reduction wave starting from 1.25 V with a peak at 0.75 V which was attributed to the formation of solid electrolyte interphase (SEI) passivation layer on the carbon electrode surface. However, intercalation/de-intercalation of lithium was presumed in the absence of any clear current peaks.
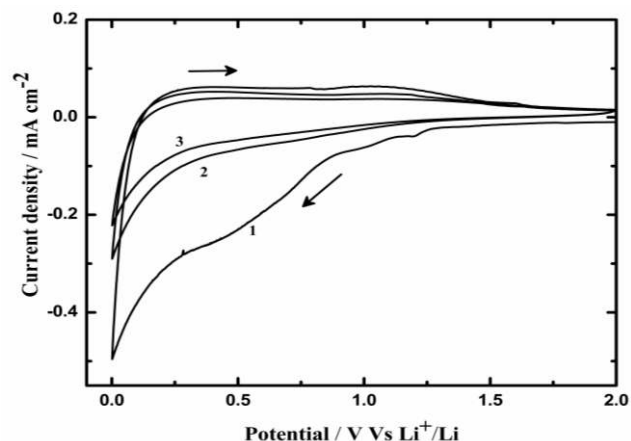

Fig. 5. Repetitive cyclic voltammograms of carbon electrode in non-aqueous electrolyte at a sweep rate of 0.05 mV s^{-1}. The number of the sweep is indicated on the corresponding curve.

The SEI layer was considered stable during the subsequent cycling, but the voltammogram became smaller in size by repeating the cycling. Cyclic voltammograms of several carbons reported by Lin *et al*. [27] are also broad in nature without clear intercalation/de-intercalation peaks. Carbons prepared from sugar cane bagasse [31], mesophase pitch [32], polymethylacrylonitrile [29], hexakis (p-bromophenyl) benzene [35], etc., provided similar voltammograms. Voltammograms recorded in the present study are similar to these studies. Formation of SEI passivation layer on the electrode causes a decrease in the voltammetric current with disappearance of even broad current peaks on repeating potential sweeps (**Fig. 5**). Insertion of Li$^+$ during cathodic sweep and extraction during anodic sweep follow as represented by reaction (1).

$$_xC + Li^+ + e^- \Longleftrightarrow LiC_x \qquad (1)$$
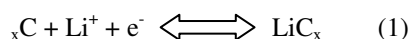
Galvanostatic charge-discharge cycling was performed between 2.0 and 0.001 V at a current density of 77 mA g^{-1}. Variation of potential with cycling is shown in **Fig. 6**. The charge capacity of the first cycle is 990 mAh g^{-1}, but the discharge capacity obtained is 400 mAh g^{-1}. Charge-discharge efficiency thus becomes only 38% for the first cycle. Irreversible capacity loss (590 mAh g^{-1}) is attributed to the formation of SEI during the first charging of the carbon electrodes [34]. The SEI formation on the electrode is a result of reaction of the electrode with the electrolyte and insoluble or partially soluble reaction products covering the electrode surface. The layer of SEI acts as an interphase between the electrode and electrolyte and it has high electronic resistivity [35]. The SEI film on the

carbon electrode slows down the kinetics of electrolyte decomposition and also reduces the consumption of active lithium by forming a physical barrier between the lithiated carbon electrode and the electrolyte. Nevertheless, the discharge capacity of 400 mAh g^{-1} obtained during the first cycle is an attractive value. The discharge capacity depends on the amount of Li stored in the carbon electrode during the charging process. Graphite intercalation compounds of composition LiC_2 and LiC_4 were synthesized under high pressure [36, 37]. These compounds are expected to provide high discharge capacities. However, they underwent decomposition to form more stable LiC_6 when pressure was reduced. On the basis of LiC_6 composition, a discharge capacity of 372 mAh g^{-1} is expected. For disordered carbons, however, discharge capacities were reported more than 372 mAh g^{-1} [36].
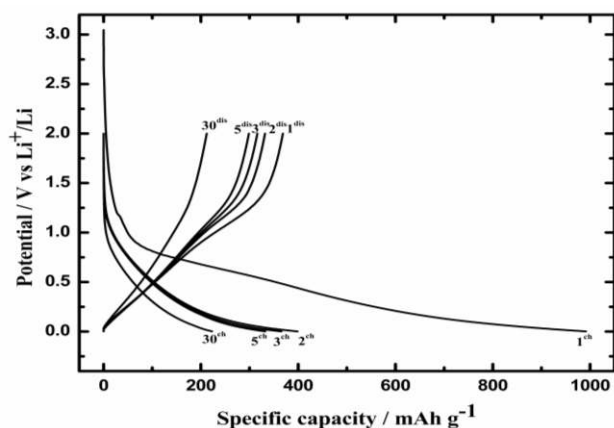
Fig. 6. Variation of potential of during charging and discharging processes at a specific current of 77 mA g^{-1} of carbon. Data of 1st, 2nd, 3rd, 5th, and 30th charge-discharge cycles are presented.
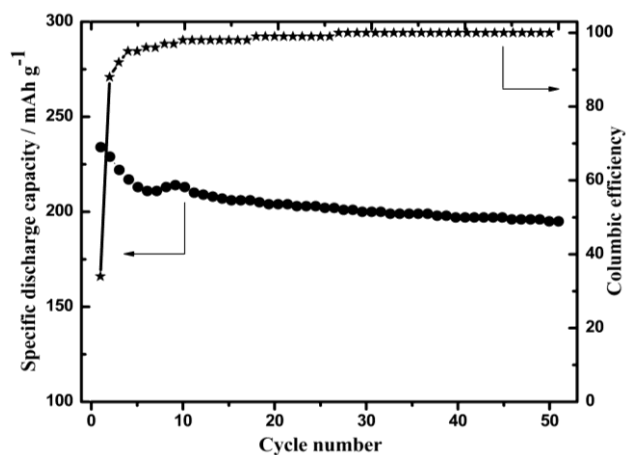
Fig. 7. Variation of discharge capacity and coulombic efficiency versus cycle number. Specific current density = 728 mA g^{-1}.

Explanations for greater discharge capacity included formation two Li layers in between two carbon layers and also excessive Li interacting with carbon at different positions in addition to interlayer distance [36, 37]. In the later explanation, three kinds of interactions between carbon and Li were considered. Li is located (i) between graphitic layers, (ii) at the edge of graphitic layers and (iii)

on the surface of crystallites. Due to the unique structure of disordered carbon, more interactions allow to store more Li compared to graphite. Thus the discharge capacity obtained for the disordered carbon in the first cycle (**Fig. 6**) is greater than the theoretically expected value from LiC_6. In the second cycle, the discharge capacity is about 330 mAh g^{-1} with coloumbic efficiency of about 80%. Cycle-life test was conducted for 50 continuous charge-discharge cycles at a specific current of 728 mA g^{-1}. A plot of discharge capacity and charge-discharge efficiency versus cycle number is shown in **Fig. 7**.

As stated above, the coulombic efficiency of cycling is about 33% in the first cycle, but it increases close to 90% in about three or four cycles and it remains at about 98% after 10 cycles. The discharge capacity is about 240 mAh g^{-1} in the first cycle. There is a gradual decrease in the capacity and 195 mAh g^{-1} is obtained at the 50th cycle with an efficiency of about 99%.

Lithium storage capacity depends on various properties of disordered carbons including the source from which the carbon is made. Zheng *et al*. [9] briefly reviewed a range of capacity values with 450 mAh g^{-1} for pyrolyzed polyfurfuryl alcohol [9], 500 mAh g^{-1} for sulfur containing carbons [9], 700 mAh g^{-1} for carbons prepared from heated pitch [9], polyparaphenylene [38], phenolic resin [37] and pitch coke [39], etc. According to the analysis of Dahn *et al*. [40], very disordered carbons consisting of a large fraction of single graphene sheets could have very large capacity of lithium due to its adsorption on both sides of the single layer sheets. This type of carbons has low voltage capacity. Furthermore, specific capacity of carbon increases with an increase in the hydrogen/carbon atomic ratio. The ratio of H/C in a carbon depends on the sources used for carbonization as well as the conditions of pyrolysis. H atoms can bind Li atoms, thus, enhancing the Li storage capability of carbons with H/C ratio. The discharge capacity of a disordered carbon with H/C atomic ratio of 0.41 was about 880 mAh g^{-1}, whereas another sample of carbon prepared from the same precursor but at a higher temperature had H/C atomic ratio of 0.04 and it delivered a capacity of only 340 mAh g^{-1}. In the present study, the high discharge capacity (400 mAh g^{-1}) obtained in the initial cycle is likely due to high H/C ratio (0.38) present in the carbon.
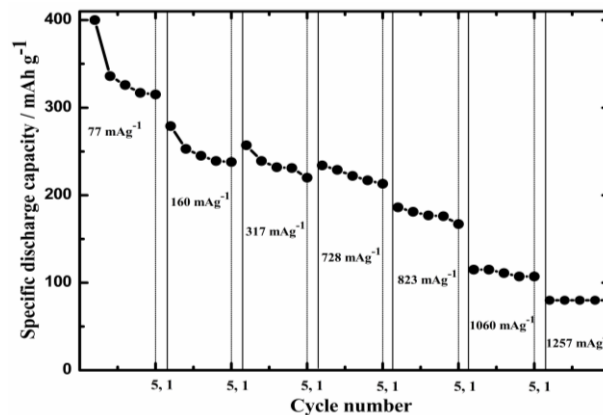

Fig. 8. Rate capability of carbon. For each rate, a separate cell is used and cycled 5 times. Specific current values used for charge-discharge are indicated.

Several cells were assembled and they were subjected to charge-discharge cycling with different currents. The results are presented in **Fig. 8**. There is a decrease in discharge capacity with an increase in rate of discharge as expected. But it is interesting to note that the carbon delivers a discharge capacity of about 80 mAh g^{-1} at specific current of 1257 mA g^{-1}. Charge-discharge studies of carbons with specific currents as high as 1257 mA g^{-1} are rarely reported in the literature. For instance, a study to suppress irreversible capacity loss occurring in the first charge-discharge cycle, Caballero *et al.* reported discharge capacity of 110 mAh g^{-1} at 2C rate for an activated carbon **[41]**. The charge-discharge specific current of 1257 mA g^{-1} is very high and a discharge capacity of 80 mAh g^{-1} at this high rate is also considered very attractive. The high rate capability of carbon prepared in the present study is likely to be due to layered structure with disordered nature. Lithium interacting with carbon on the surface and edges can undergo fast discharge and charge resulting in high rate capability.

Diffusion coefficient of Li$^+$ (D$_{Li}^+$) in carbon was estimated by GITT method **[42]**. A carbon electrode was subjected to lithiation by applying a constant current (I$_0$) for a time, τ. There was a gradual change in its potential from its equilibrium value (E$_0$) to E$_\tau$ at time τ (**Fig. 9A**).
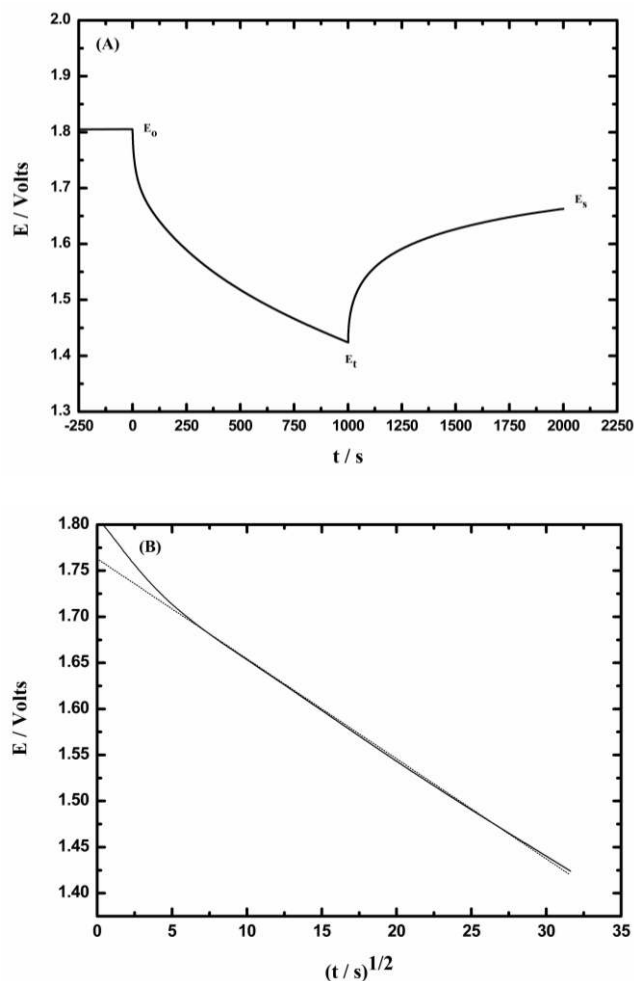
After interruption of current at time τ, the electrode was allowed to reach its new steady-state potential, E$_s$. The change in its steady-state potential, ΔE$_s$ (=E$_s$-E$_o$) was calculated, **Fig. 9A**. The potential decreases linearly with t$^{1/2}$ as shown in **Fig. 9B** during charging. From the values of ΔE$_\tau$ (=E$_\tau$ - E$_o$) and ΔE$_s$, (D$_{Li}^+$) was calculated using Eq. (2).

$$D_{Li+}= (4/(\pi\tau))(m_B V_M/M_B A)^2(\Delta E_s/\Delta E_\tau)^2 \qquad (2)$$

where m$_B$ is the mass of active material, M$_B$ is molar mass, V$_M$ is molar volume and A is area of the electrode. The value of (D$_{Li}^+$) obtained is 6.7×10^{-12} cm^2 s^{-1}. This value is comparable with values of (D$_{Li}^+$) reported in several other carbons **[43]**.

Conclusion

Disordered carbon is made from coconut kernel, which is free from milk, by heating at 600 $^\circ$C in N$_2$ atmosphere. The inter-layer distance obtained from (002) reflection of powder XRD pattern is 3.80 Å. A layer like morphology is observed in SEM and TEM images. Charge-discharge studies suggest an initial discharge capacity of 400 mAh g^{-1} with an irreversible capacity of 590 mAh g^{-1}. Fairly stable discharge capacity is measured on repeated cycling. The electrodes withstand charge-discharge specific current as high as 1257 mA g^{-1} and they deliver a discharge capacity of 80 mAh g^{-1}. The high rate capability of carbon is considered as an important property for fast charging of Li-ion batteries.

Reference

1. Wakihara, M. *Mater Sci Eng: Reports*. **2001**, *33*, 109. **DOI:** 10.1016/s0927-796X(01)00030-4,
2. Noel, M.; Suryanarayanan, MV. *J . Power Sources*. **2002,** *111*, 193. **DOI:** 10.1016/s0378-7753(02)00308-7
3. Tiwari, A.; Valyukh, S. (Eds.), Advanced Energy Materials, Wiley-Scrivener Publishing, USA, **2014**. **ISBN:** 978-1-118-68629-4
4. Fong, R,; Von Sacken, U,; Dahn, JR. *J . Electrochem. Soc.* **1990,** *137*, 2009. **DOI:** 10.1149/1.2086855
5. Zheng, T,; Zhong, Q,; Dahn, JR. *J. Electrochem. Soc.* **1995,** *142*, L211. **DOI:** 10.1149/1.2048450
6. Huang, B,; Huang, Y,; Wang, Z,; Chen, L,; Xue, R,; Wang, F. *J. Power Sources*. **1996,** *58,* 231. **DOI:** 10.1016/s0378-7735(96)02373-7
7. Gong, J,; Wu, H. *Electrochim Acta* **2000**, *45,* 1753. **DOI:** 10.1016/s00134686(99)00400-4
8. Jung , Y,; Suh, MC.; Lee, H,; Kim, M,; Lee, SI,; Shim, SC,; Kwak, J. *J. Electrochem. Soc,* **1997**, *144,* 4279. **DOI:** 10.1149/1.1838179
9. Zheng, T,; Liu, Y,; Fuller, EW,; Tseng, S,; Von Sacken, U,; Dahn, JR. *J. Electrochem. Soc.* **1995,** *142,* 2581. **DOI:** 10.1149/1.2050057
10. Leroux, F,; Meternier, K,; Gautier, S,; Frackowiak, E,; Bonnamy, S,; Beguin, F. *J. Power Sources.* **1999**, *81/82,* 317. **DOI:** 10.1016/s0378-7753(99)00130-5
11. Fey, GTK,; Kao, YC. *Mater. Chem. Phy.* **2002,** *73,* 37. **DOI:** 10.1016/s0254-0584(01)00348-0

Fig. 9 (A). Variation of potential with time (t) when a charging current of 10 μA injected at E$_o$ and terminated at E$_\tau$; and (B). Linear variation of potential with square root of time during charging step.

12. Xing, W.; Xue, JS.; Dahn, JR. *J. Electrochem. Soc.* **1996**, *143,* 3046.
    DOI: 10.1149/1.1837162
13. Fey, GTK.; Chen, KL.; Chang, YC. *Mater. Chem . Phy.* **2002,** *76,* 1.
    DOI: 10.1016/s0254-0584(01)00495-3
14. Buiel, E.; George, EA.; Dahn, JR. *J . Electrochem. Soc.* **1998**, *145,* 2252.
    DOI: 10.1149/1.1838629
15. Fey, GTK.; Chen, CL. *J. Power Sources.* **2001,** *97-98,* 47.
    DOI: 10.1016/s0378-7753(01)00504-3
16. Guo, Y.; Yang, S.; Yu, K.; Zhao, J.; Wang, Z.; Xue, H. *Mater. Chem. Phy.* **2002**, *74,* 320.
    DOI: 10.1016/0254-0584(01)00473-4
17. Li, W.; Chen, M.; Wang, C. *Mater. Lett.* **2011**, *65,* 3368.
    DOI: 10.1016/j.matlet.2011.07.072
18. Stephan, AM.; Premkumar, T.; Ramesh, R.; Thomas, S.; Jeong, SK.; Nahm, KS. *Mater. Sci. Eng. A.* **2006**, *430,* 132.
    DOI: 10.1016/j.msea.2006.05.131
19. Hwang, YJ.; Jeong, KS.; Nahm, KS.; Shin, JS.; Stephan, AM. J. Phy. Chem. Solids. **2007**, *68,* 182.
    DOI: 10.1016/j.jpcs.2006.10.007
20. Fey, GTK.; Lee, DC.; Lin, Y.; Premkumar, T. *Synth. Met.* **2003**, *139,* 71.
    DOI: 10.1016/s0379-6779(03)00082-1
21. Hwang, YJ.; Jeong, SK.; Shin, JS.; Nahm, KS.; Stephan, AM. *J. Alloys. Comp.* **2008**, *448,* 141.
    DOI: 10.1016/j.jallcom.2006.10.036
22. Zhou, P.; Lee, R.; Claye, A.; Fischer, JE. *Carbon.* **1996**, *36,* 1777.
    DOI: 10.1016/s0008-6223(98)00126-2
23. Dahn, JR.; Sleigh, AK.; Reimers, JN.; Zhong, Q.; Way, BM. *Electrochim. Acta.* **1993**, *38,* 1179.
    DOI: 10.1016/0013-4686(93)80048-5
24. Gong, J.; Wu, H.; Yang, Q. *Carbon.* **1999**, *37,* 1409.
    DOI: 10.1016/s0008-6223(99)00002-0
25. Tuinstra, F.; Konig, JL. *J. Chem. Phy.* **1970**, *53,* 1126.
    DOI: 10.1063/1.674108
26. Yi, Z.; Liang, Y.; Lei, X.; Wang, C.; Sun, J. *Mater. Lett.* 2007, *61,* 4199.
    DOI: 10.1016/j.matlet.2007.01.054
27. Lin, ZJ.; Hu, XB.; Huai, YJ.; Deng, ZH. *J. Serbian. Chem Soc.* **2010**, *75,* 271.
    DOI: 10.2298/JSC1002271L

28. Yi, Z.; Han, X.; Ai, C.; Liang, Y.; Sun, J. *J. Solid State. Electrochem.* **2008**, *12,* 1061.
    DOI: 10.1007/10008-007-0427-9
29. Guidotti, R.; Johnson, B. *Proceedings of IEEE.* 193, **1996**.
30. Kim, MS.; Fang, B.; Kim, JH.; Yang, D.; Kim, YK.; Bae, TS.; Yu, JS. *J. Mater. Chem.* **2011**, *21,* 19362.
    DOI: 10.1039/C1JM13753K

31. Matsubara, EY.; Lala, SM.; Rosolen, JM. *J. Brazilian. Chem .Soc.* **2010**, *21,* 1877.
    DOI: 10.1590./s0103-50532010001000012
32. Hou, Z.; Zeng, F.; He, B.; Tao, W.; Ge, C.; Kuang, Y.; Zeng, J. *Mater. Lett.* **2011**, *65,* 897.
    DOI: 10.1016/j.matlet.2010.12.008
33. Bonino, F.; Brutti, S.; Piana, M.; Scrosati, B.; Brambilla, L.; Fustella, G.; Castiglioni, C.; Zerbi, G.; Zane, D.; Renouard, T.; Mathis, C. *J. Electrochem. Soc.* **2005**, *152,* A2023.
    DOI: 10.1149/1.2018627
34. Aurbach, D.; Teller, H.; Levi, E. *J. Electrochem. Soc.* **2002**, *149,* A1255.
    DOI: 10.1149/1.1502683
35. Peled, E.; Golodnitsky, D.; *SEI on lithium, graphite, disordered carbons and tin based alloys : In* Lithium-ion batteries: Soild-electrolyte interphase*;* Balbuena, P.B.; Wang, Y. (Eds.); Imperial College Press Publication: London, **2004,** pp. 1-69.
36. Matsumura, Y.; Wang, S.; Mondori, J. *Carbon.* **1995**, *33,* 1457.
    DOI: 10.1016/0008 6223(95)00098-X
37. Nalimova, VA.; Semenenko, KN. *Carbon .* **1994**, *32,* 1019.
    DOI: 10.1016/0008-6223(94)90063-9
38. Yata, S.; Kinoshita, H.; Komori, M.; Ando. N.; Kashiwamura, T.; Harada, T. *Synt.Met.* **1994**, *62,* 153.
    DOI: 10.1016/0379-6779(94)90306-9
39. Sato, K.; Noguchi, M.; Demachi, A.; Oki, N.; Endo, M. *Science.* **1994**, *264,* 556.
    DOI: 10.1126/science.264.5158.556
39. Iijima, T.; Suzuki, K.; Matsuda, Y. *Synth. Met.* **1995**, *73,* 9.
    DOI: 10.1016/0379- 6779(95)03290-8
40. Liu, Y.; Xue, JS.; Zheng, T.; Dahn, JR. *Carbon.* **1996**, *34,* 193.
    DOI: 10.1016/00086223(96)00177-7
41. Caballero, A.; Hernán, L.; Morales, J.; Olivares-Marin, M.; Gómez-Serranob, V. *Electrochem. Solid-State. Lett.* **2007**, *12,* A167.
    DOI: 10.1149/1.3143922
42. Weppner, W.; Huggins, RA. *J. Electrochem. Soc.* **1977**, *124,* 1569.
    DOI: 10.1149/1.2133112
43. Uchida, T.; Morikawa,Y.; Ikuta, H. Wakihara M. *J. Electrochem. Soc.* **1996,** *143,* 2606.
    DOI: 10.1149/1.1837055